POLITECNICO DI TORINO
Repository ISTITUZIONALE

Hydraulic Characterization of Solenoid-actuated Injectors for Diesel Engine Common Rail Systems

(Article begins on next page)

20 April 2024

Hydraulic characterization of solenoid-actuated injectors for diesel engine Common Rail systems.

Ferrari A.[a],*, Mittica A.[a], Paolicelli F.[a], Pizzo P.[a]

[a]Politecnico di Torino, Corso Duca degli Abruzzi, 24, Torino, 10129, Italy

Abstract

Injection systems represent key elements in modern diesel engines because of the fundamental role played in fuel spray formation and evolution during the combustion phase. For this reason, their design needs attention and continuous improvements in order to satisfy environmental standards and consumer demands. The present work illustrates the main phases that form the basis of an activity of hydraulic characterization of a solenoid injector for diesel engine applications. The performance of the injection system has been verified by means of injected flow-rate time histories, fuel injected quantities, leakages through the injector pilot-valve, electric driving signals and pressure transients, for different operating conditions, which refer to single and multiple injections. Furthermore, a complete numerical model of the injector and of the high-pressure hydraulic circuit of the injection apparatus has been developed with the aim of deepening the understanding of the internal dynamics of the injection system, which could not be analyzed only experimentally.

Keywords: Common Rail; solenoid-actuated diesel injectors; hydraulic characterization; injector numerical model.

1. Introduction

   Modern injection systems for diesel engines are required to guarantee accurate fuel metering, control of the injection rate and high capability to manage different injection strategies, such as closely-coupled multiple injections, boot and ramp shaped main injections [1]. All these factors play a fundamental role in the fuel spray

* Corresponding author. Tel.: +39-011-090-4426;
   E-mail address: alessandro.ferrari@polito.it

formation and evolution inside the combustion chamber. Furthermore, the efficiency of the air-fuel mixing process and the subsequent combustion development depend on the injection event, which can significantly affect combustion noise, engine performance and pollutant formation [2-4]. In order to improve the injection system performance, an accurate analysis of the injector hydraulic behavior is required, since it allows the potential weak points in the injection apparatus to be determined. The injector characterization has to be carried out during transient operations as well as under quasi-steady state conditions. In the first case, injector opening and closure phases, and very short energizing times (*ET*s) are performed, while the latter circumstance is achieved by long injection durations and full needle lift [5]. In the present work, an assessment of the system has also been made during multiple injection pulses, with the aim of deepening the knowledge of the influence that pressure waves, which are triggered by the first injection shot and that propagate inside the high-pressure circuit of the apparatus, can have on the subsequent injection events in terms of injected fuel amount. The primary objective of the work is to provide some guidelines for a complete experimental-numerical characterization of the injector. In this perspective, some of the experimental results, which highlighted possible anomalies, have been compared with numerical results. The numerical investigation represents in fact a valuable support for the improvement of the injector hydraulic performance, since it allows to analyze the cause-effect relationships which feature the main nonstationary events related to the injector working.

Nomenclature

A	orifice cross-section
C	discharge flow coefficient
CR	Common Rail
DT	dwell time between consecutive injection shots
ECU	electronic control unit
ET	energizing time
EMI	injection quantity indicator (Einspritzmengenindikator)
EVI	injection rate indicator (Einspritzverlaufsindikator)
FMV	fuel metering valve
G	mass flow rate
ICEAL	internal combustion engine advanced laboratory
KMM	continuous flow-rate meter
l_n	needle lift
M	fuel mass
NCD	nozzle closure delay
NOD	nozzle opening delay
p	fuel pressure
PT	Politecnico di Torino
t	time
V	fuel volume
δ	volume variation (injector-to-injector)
ρ	fuel density
σ	volume variation (cycle-to-cycle)

Subscripts

0	initial value
after	after injection
inj	injected (mass), injector inlet (pressure)
main	main injection
max	maximum
min	minimum
nom	nominal

num	numerical
rail	rail pressure
ref	value used for normalization
tot	total

2. Experimental set up and facility

The experimental campaign on the Common Rail (*CR*) injection system has been performed at the Moehwald-Bosch hydraulic test bench installed in the ICEAL-PT (Internal Combustion Engine Advanced Laboratory at the Politecnico di Torino) [6]. The *CR* injection system that has been employed for the experimental tests is made up of a high-pressure volumetric pump, a rail with an internal volume of 20 cm^3 and four injectors. The system can work at a maximum operating pressure of 1600 bar. The injectors are indirect-acting servo solenoid-actuated, equipped with a standard pilot-valve and a mini-sac type, which features 8 injection holes. The high-pressure pump has two inline pistons. Each pumping element is equipped with a fuel metering valve (*FMV*), which is actuated by the *ECU* to regulate the pump delivered flow-rate and control the rail pressure level (p_{rail}). The latter is detected by means of a pressure sensor installed at one rail extremity. A piezoresistive transducer has been installed on one of the rail-to-injector pipes for the acquisition of the pressure trace at the injector inlet (p_{inj}). In the performed tests, the *EMI2* flowmeter [6] has been used to measure the injected mass in single injections, as well as in each shot of the multiple injection trains. The *EVI* flowmeter [6] has been used to detect the instantaneous injected flow-rate, while the fuel leakages have been detected by means of the *KMM* continuous measuring flow meter. The investigation has involved a wide range of engine-like conditions. Single shots have been realized in the 300-1600 bar range of p_{nom} and in the 0.35-1.2 ms range of *ET*, at a pump speed of 1000 rpm, which corresponded to an engine speed of 2000 rpm. Multiple injections, such as pilot-main and main-after, have covered a sweep of dwell time (*DT*) from 0.3 ms to 3.1 ms, within the same range of p_{nom} and *ET* as the ones used for single injections.

3. Injector numerical model and validation

A one-dimensional numerical model of the injector has been developed to support the experimental analysis. The model is essentially composed of three modules corresponding to the injector pilot-valve, the needle and the nozzle. The experimental p_{rail} time history together with the current and voltage signals, which provide the magnetic force to the pilot-valve, are required as input data. The p_{rail} time evolution allows the rail pressure control system action and the high-pressure pump dynamics to be taken into account, whereas the current and voltage signals are used to calculate the magnetic force to the pilot-valve. For the validation of the model, two outcomes have been compared with the experimental data: the injected flow rate (G_{inj}) and the pressure at the injector inlet (p_{inj}).
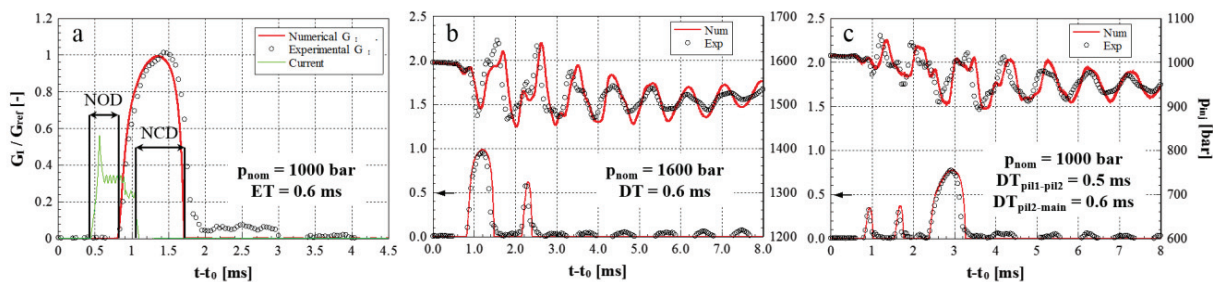

Fig. 1. Numerical model validation for (a) a single injection, (b) a main-after and (c) a pilot-pilot-main injection.

Figure 1 reports the obtained results for some of the operating conditions that have been explored. As can be observed in the plots, the model is able to predict the injector behavior with a satisfactory level of accuracy. The injector internal dynamics can therefore be studied in order to better understand the cause-and-effect relationships during the transient operations and deepen the knowledge of some experimentally observed phenomena.

4. Single injections characterization

The injector hydraulic characteristics, reported in Fig. 2, show the amount of fuel that an injector is able to deliver for each operative condition, determined by the ET value and p_{nom} level. The influence of the pressure level on the injected fuel quantity V_{inj} can be roughly interpreted on the basis of the following equation, whose integration term is often used for defining the flow through nozzles and orifices:

$$V_{inj} = \int_{t_0}^{T} C \cdot A \sqrt{\frac{2\Delta p}{\rho}} dt \tag{1}$$

where C is the discharge flow coefficient, A the restricted flow-area, which also depends on the needle lift l_n, ρ the fuel density and $\Delta p = p_{nom} - p_0$ represents the difference between the nominal pressure level (p_{nom}) and the pressure level in the chamber (p_0) where injection occurs, T is the duration of the injection event, which is related to ET. In general, the higher p_{nom}, the higher the injected quantity at fixed ET value.
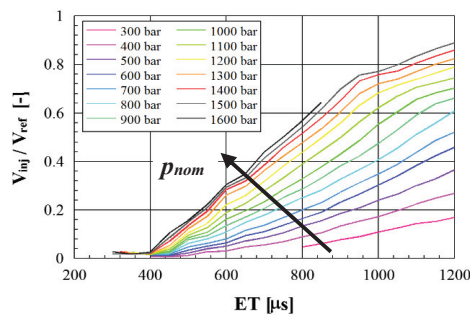

Fig. 2. Injector hydraulic characteristics.

The results in Fig. 2 also show that the injector hydraulic behavior is partially linear with respect to ET. A first change in the curve slop can be observed at lower ETs (around 400 μs in Fig. 2). This change can be attributed to the variation of the restricted flow area. In fact, when the injection duration is long enough, the restricted section moves from the needle-seat passage to the nozzle injection holes. A second change in the slope of the injector characteristics can occur if the needle stroke-end is reached, while the slope does not vary if the needle is ballistic. The ET value at which this second change in slope occurs is related to the p_{nom} level since it influences the needle upward velocity, thus the restricted flow-area time variation. Actually, the flow-area increasing rate is higher before the needle stroke-end is reached. This event has been confirmed by the numerical tests presented in Fig. 3.
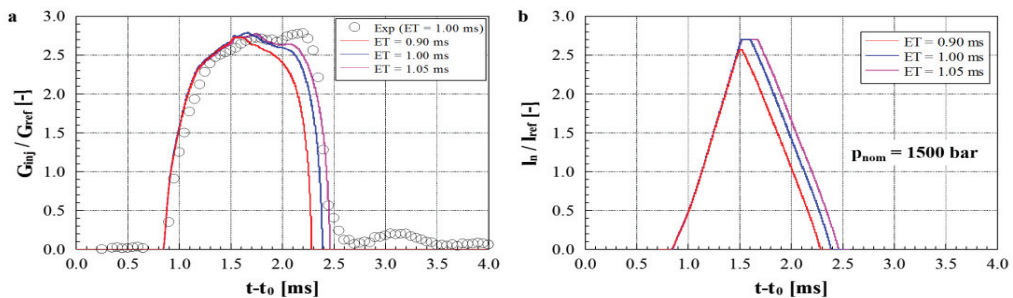

Fig. 3. (a) Injected flow rate; (b) needle lift.

Figure 3a reports the injected flow-rate for three different ET values, while the corresponding needle lift is shown in Fig. 3b. The change in slope of the curves plotted in Fig. 2 happens when the needle reaches its stroke-end, that

is, starting from about $ET = 0.95$ ms, at $p_{nom} = 1500$ bar, in Fig. 3. From this point on, the increasing in the restricted flow-area is lower and therefore the injector characteristic slope is reduced.

4.1. Injected fuel quantity dispersion

Cycle-to-cycle fluctuations in injected fuel volume are usually due to fluid dynamics and mechanical events. Two possible causes of dispersion can be identified by means of the injection profile analysis: fluctuations of the profile maximum values and of the flow-rate slope at the beginning of the injection. In the first case, the cause can be the nozzle design, while, in the latter, the pilot-valve design or the needle kinematics can be responsible. The *ECU* can also influence a stable behavior of the injection apparatus, since it has to provide stable and repeatable electric command signals to the injector. The volume dispersion has been computed as deviation from the mean injected volume, $\overline{V}_{main}$, over 100 injections, at fixed working conditions, as follows:

$$\sigma = \frac{V_{main} - \overline{V}_{main}}{\overline{V}_{main}} \cdot 100 \tag{2}$$

where V_{main} is the volume of fluid injected during a main injection event. The 3D bar chart in Fig. 4 reports the deviation with respect to both p_{nom} and ET values. As can be observed, the considered injector is generally characterized by low cycle-to-cycle dispersion. The highest values of σ pertain to the smallest injected quantities. In general, the cycle-to-cycle dispersion should be lower than the 3-5% for automotive applications.

Dispersion in injected fuel volumes also exist among injectors from the same manufacturer. The variability of the production process also can affect the injector performance. For this reason, the fuel quantities, injected by a statistical group of injectors at the same working conditions, should be evaluated. In the present work, the so-called injector-to-injector variation, δ, has been computed as the difference between the largest, V_{max}, and the smallest, V_{min}, injected fuel volume, over the mean injected volume, $\overline{V}$, as follows:

$$\delta = \frac{V_{max} - V_{min}}{\overline{V}} \cdot 100 \tag{3}$$

The outcomes, reported in Fig. 5, show that the variability generally reduces with increasing values of p_{nom} and ET; in fact, the control of tiny quantities is commonly known to be more demanding.
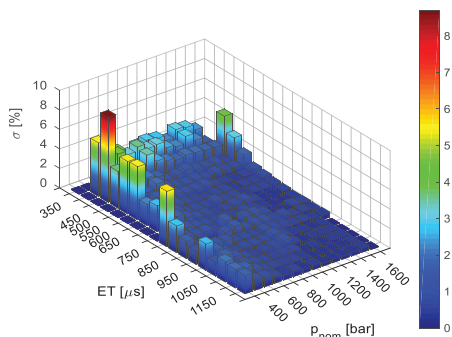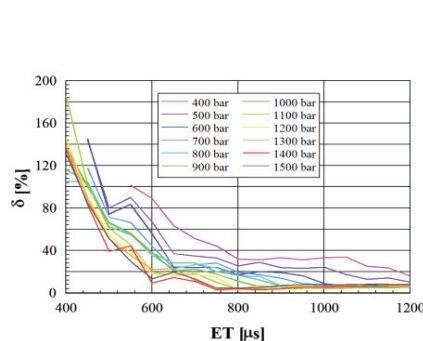

Fig. 4. Cycle-to-cycle dispersion.

Fig. 5. Injector-to-injector variation.

4.2. Injection rate

The study of the injection profiles allows to observe how it modifies as ET or p_{nom} changes. Potential anomalies in the injector performance can therefore be identified. Some examples of the investigated cases are reported in Figs. 6-7, which report the p_{EVI} trace, that is, the pressure variation detected by the *EVI* meter (here normalized), for different ET values at fixed p_{nom} level (Fig. 6) and vice versa (Fig. 7). As can be observed, in Fig. 6 an increase in

the flow rate has been detected at the end of the injection profiles for high p_{nom} and $ET > 1$ ms. As far as the curves reported in Fig. 7 are concerned, the injection rate uniformly progresses with p_{nom} at small ETs (0.6 ms in the case in figure), while for large ETs it has been noted to become more irregular as p_{nom} grows.
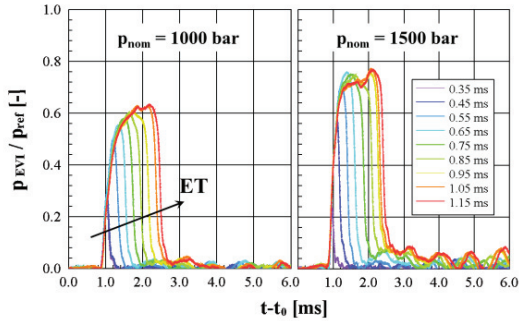

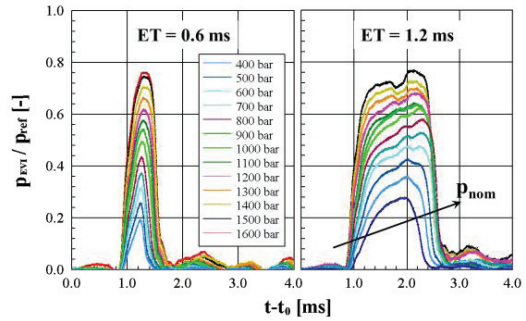Fig. 6. Injection profiles as *ET* changes.

Fig. 7. Injection profiles as p_{nom} changes.
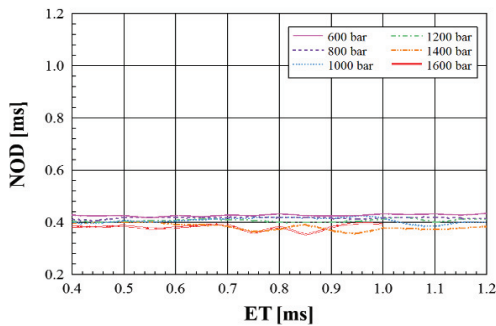
4.3. Nozzle opening and closure delays

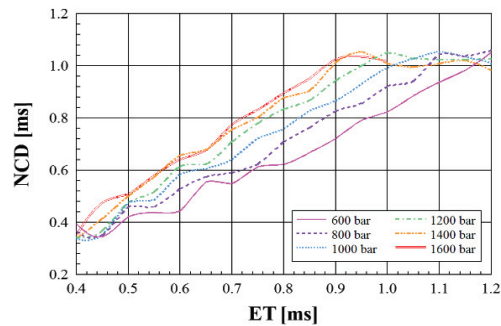Fig. 8. Injector nozzle opening delays.

Fig. 9. Injector nozzle closure delays.

The *NOD* (Nozzle Opening Delay) is the time interval between the start of the electric command signal to the injector pilot-valve and the instant at which the fuel injection begins. The *NCD* (Nozzle Closure Delay) is instead the period between the end of the electric command signal and the instant at which the nozzle closes. The dependence of these two parameters on p_{nom} and ET is shown in Figs. 8-9, respectively. As can be observed, *NOD* is quite constant with ET and a minimum variation occurs with p_{nom}. *NCD* is widely affected by ETs and p_{nom} levels and it rises as either ET or p_{nom} increases. If the needle is not ballistic, it stabilizes around a certain value (1 ms in the present case) as the needle reaches its stroke-end. Since *NCD* is larger than *NOD*, the time interval during which the fuel is injected, that is, the injection hydraulic duration, results to be greater than ET, especially for large injections.

4.4. Injector static and dynamic leakages

Indirect-acting injectors have to be characterized also in terms of fuel leakages. An amount of fuel is in fact lost during the injector operation, even when the injector is not energized because of the pilot-valve sealing and of the injector clearances between control piston and its sleeve [7]. Figure 10 shows the static leakages, measured as fuel volumes per engine cycle, at fixed temperature of about 40 °C and atmospheric pressure, when the injector solenoid is not energized ($ET = 0$). As can be observed, a relevant increasing trend with p_{nom} characterizes this type of injectors, especially at high p_{nom} values. Such behavior can be related to the unbalanced ball-type pilot-valve layout and to the increase of the fuel temperature, which is due to fuel throttling across the leakage path [7]. In Fig. 11 the

total leakage (with solid line) and the dynamic leakage (with symbols) are plotted: the former is detected during the injector operation, while the latter is obtained as difference between total and static leakages.
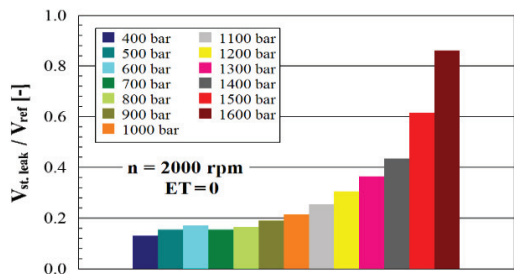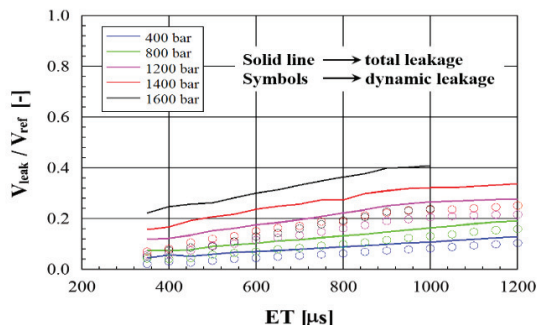

Fig. 10. Injector static leakages.

Fig. 11. Injector total and dynamic leakages.

5. Multiple injection characterization

A fundamental issue for modern *CR* injectors is represented by the capability of performing multiple injection shots during an engine cycle. In this scenario, the dependence of the injection system performance on *DT*, that is, the time interval between the electrical commands of two consecutive injection events, has to be investigated in detail in terms of injected quantities and deviation. Tests have been carried out with pilot-main and main-after injections. Figures 12a and 12b report the injected flow-rate detected for two different pressure levels (p_{nom} = 600 bar and p_{nom} = 1400 bar) when pilot-main injection shots are performed. The *DT* between the two injection events has been reduced from 3.1 ms to 0.1 ms in steps of 200 μs. It is shown that the pilot injection is practically the same for all the tests, whereas the maximum value of the *EVI* curve related to the main injection varies as the injection start is moved. This phenomenon can be explained by analyzing the p_{inj} time history. The pilot injection event generates pressure waves, which propagate from the nozzle towards the rail and travel back and forth in the high-pressure circuit. Such pressure waves influence the following injection since, according to the considered *DT* value, the main shot can take place in correspondence of a local minimum or a local maximum of p_{inj} and this causes differences in the injected flow-rate peak. The effects on injected quantities are shown in Figs. 13a and 13b, these have been reported as a function of *DT* for the two considered pressure levels.
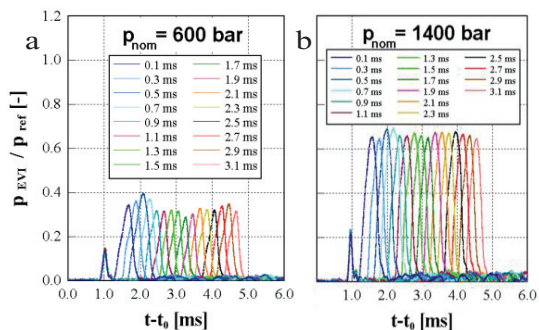

Fig. 12. EVI curves for pilot-main injection pattern:
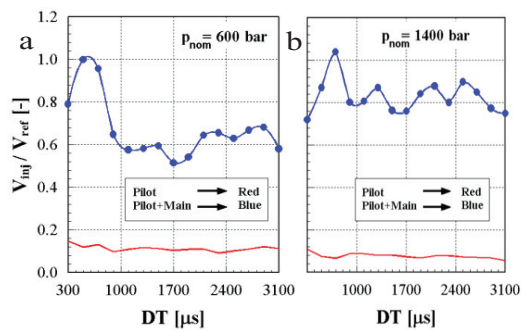(a) p_{nom} = 600 bar, (b) p_{nom} = 1400 bar.

Fig. 13. Injected quantity variation vs. DT:
(a) p_{nom} = 600 bar, (b) p_{nom} = 1400 bar.

With regard to main-after injection schedules, Fig. 14 reports data of two different pressure levels: p_{nom} = 800 bar (Fig. 14a) and p_{nom} = 1000 bar (Fig. 14b). As can be observed, the influence of *DT* on the second shot is more significant in main-after schedules than in pilot-main schedules, because the pressure waves triggered by the main injection are more intense than those triggered by the pilot injection. Furthermore, the pressure values exert a higher influence on an injection with short *ET*, such as an after shot, than on the main injection.
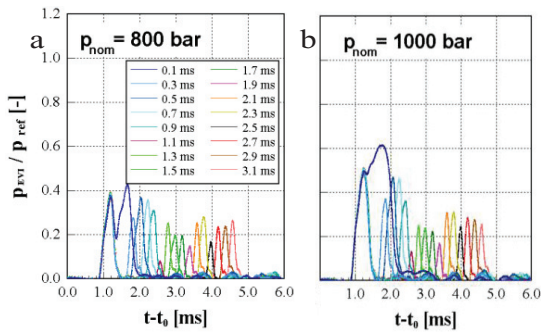
Fig. 14. EVI curves for main-after injection pattern:
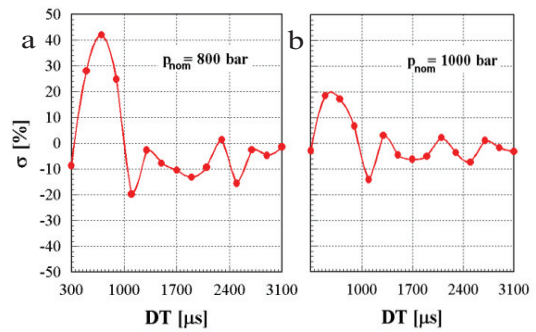(a) p_{nom} = 800 bar, (b) p_{nom} = 1000 bar.

Fig. 15. Total injected volume variation vs. DT:
(a) p_{nom} = 800 bar, (b) p_{nom} = 1000 bar.

Figure 15 shows the total injected quantity (V_{tot} = V_{main} + V_{after}), reported in terms of σ, evaluated by means of an analogous relation to Eq. 2. V_{tot} oscillates as the *DT* value is changed because of the variation in the after injection quantity, since the main injection is virtually unaffected by *DT*. Furthermore, it has been found that injection fusion occurs as the *DT* is reduced below 0.2 ms for all the tested pressure level (this *DT* value is referred to as injection fusion threshold). In these conditions, the second injection shot starts before the first one has finished and it is not possible to distinguish the two injection events; moreover, the total injected quantity grows remarkably compared to longer *DT* values.

6. Conclusions

The procedure for a complete hydraulic characterization of an injector for *CR* diesel applications has been outlined for a solenoid-actuated injector. The analysis of the single injection tests has revealed that the dependence of the injected fuel volume on the *ET* value at fixed p_{nom} is practically linear once the restricted flow-area has passes from the needle-seat passage to the nozzle holes. However, a change in the slope of the injector characteristics takes place at higher *ET* values as the needle reaches its stroke-end. The injection rate curves have been used to evaluate the nozzle opening and closure delays: the former has been found to be almost independent from *ET* and p_{nom} values, whereas the latter features a significant dependence on both these parameters. The injection rate curves can be also used to investigate possible causes of cycle-to-cycle and injector-to-injector dispersion. The injector static leakages have been found to be significantly influenced by the nominal pressure level and this can be related to the pilot-valve layout and also to the increase in fuel temperature. The analysis of multiple injection patterns shows that the pressure waves triggered by the first injection shot can affect the injected fuel quantity of the next shots as the *DT* varies. In the case of main-after injections, this effect is more significant than in pilot-main injections, because the first shot is larger than the latter and the intensity of the triggered pressure wave is higher.

References

[1] Benajes J, Molina S, De Rudder K, Rente T. Influence of injection rate shaping on combustion and emissions for a medium duty diesel engine. *Journal of Mechanical Science and Technology*, 2006; 20(9):1436-1448.

[2] Hyun K S. Investigation of multiple injection strategies for the improvement of combustion and exhaust emissions characteristics in a low compression ratio (CR) engine. Applied Energy, 2011;88(12):5013-5019. 36, 2004.

[3] Busch S, Zha K, Miles PC. Investigation of closely coupled pilot and main injections as a means to reduce combustion noise in a small-bore direct injection Diesel engine. *International J of Engine Research*, 2015,16(1):13-22.

[4] Mulemane A, Han JS, Lu PH, Yonn SJ, Lai MC. Modeling Dynamic Behavior of Diesel Fuel Injection Systems. SAE Paper 2004–01-05

[5] Payri R, Salvador FJ, Gimeno J, De la Morena J. Influence of injector technology on injection and combustion development – Part 1: Hydraulic characterization. Applied Energy, 2011;88:1068-1074.

[6] Catania AE, Ferrari A, Manno M, Spessa E. Experimental Investigation of Dynamics Effects on Multiple-Injection Common Rail System Performance. ASME. J. Eng. Gas Turbines Power 2008;130(3):032806-032806-13.

[7] Ferrari A, Paolicelli F, Pizzo P. The new generation of solenoid injectors equipped with pressure-balanced pilot valves for energy saving and dynamic response improvement. Applied Energy, 2015;151:367-376.